Waste Management 174 (2024) 15–23

Contents lists available at ScienceDirect

Waste Management

journal homepage: www.elsevier.com/locate/wasman

Research Paper

Sorption and diffusion of per-polyfluoroalkyl substances (PFAS) in high-density polyethylene geomembranes

Aamir Ahmad [a], Kuo Tian [a,*], Burak Tanyu [a], Gregory D. Foster [b]

[a] Department of Civil and Environmental Engineering, George Mason University, Fairfax, VA, 22030, USA
[b] Department of Chemistry & Biochemistry and Potomac Environmental Research and Education Center at PSC, George Mason University, Woodbridge, VA, 22191, USA

ARTICLE INFO

Keywords:
Sorption
Diffusion coefficient
PFAS
PFCAs
PFSAs
Gen X
HDPE

ABSTRACT

The objective of this study is to investigate the fate and transport of per-polyfluoroalkyl substances (PFAS) through a high-density polyethylene (HDPE) geomembrane (GM) that is commonly used in landfill composite liner systems. Tests were conducted to measure the sorption and diffusion of per-polyfluoroalkyl substances (PFAS) with varying number of carbons in chain and functional groups on HDPE GM. Perfluoroalkyl carboxyl acids (PFCAs), perfluoroalkyl sulphonic acids (PFSAs), alkyl-sulfonamidoacetic acids (FOSAAs), fluorotelomer sulfonic acids (FtSAs), alkane sulfonamides (FOSA) and ether carboxylic acids (Gen X) were investigated in this study. The partition coefficients (K_d) on HDPE GM ranged from 3.8 to 98.3 L/kg. PFAS with amide and sulfonic functional groups showed stronger sorption than that of PFAS with carboxylic acid functional groups. Molecular weight directly affected the K_d for long-chained PFAS whereas the K_d of short-chained PFAS was not sensitive to molecular weight. The diffusion coefficients (D_g) of PFCAs and PFSAs through 0.1-mm HDPE GM were found to be in the orders of 10^{-18} to 10^{-17} m^2/s. The D_g decreased with increasing molar mass and were also observed to be dependent on the functional group. D_g of PFSAs was lower than that of PFCAs for similar number of carbons in the chain. The estimated mass flux for PFAS in an intact 1.5-mm HDPE GM varied from 38.7 to 2080.8 ng/m^2/year whereas the estimated diffusive breakthrough time for PFAS in intact 1.5-mm HDPE was 1526 years or longer.

1. Introduction

High-density polyethylene (HDPE) geomembranes (GM) are an integral component of a composite landfill liner (Koerner and Koerner (2006); Nefso and Burns, 2007; Rowe, 2005) to reduce the transport of contaminants from municipal solid waste (MSW) landfill leachate into the subsoil/groundwater (Foose et al., 2002). HDPE GMs are primarily composed of polyethylene resin, which is a thermoplastic polymer (Nefso and Burns, 2007; Rowe, 2005;Tian et al., 2017). In addition to the resin antioxidants, stabilizers, and UV absorbers are also incorporated into the GM to enhance mechanical properties (e.g., tensile strength, tear, and puncture resistance) and make it resistant to chemicals, UV degradation, and weathering (August and Taztky (1984); Hsuan and Koerner, 1995; Tian et al., 2018).

HDPE GMs consist of non-polar molecules and provide an excellent impedance to the advective migration of contaminants by the reduction of water flow. HDPE GMs also act as an ideal barrier to the diffusive transport of inorganic (polar) contaminants (Rowe et al., 1995). However, non-polar organic contaminants can migrate through intact HDPE GMs by diffusion (Aminabhavi and Naik, 1998; Rowe et al., 1996). This migration process through an HDPE GM can be broken down into three processes, which include (I) the sorption of the contaminant from the landfill leachate to the upper layer of the GM, (II) the diffusion of the contaminant through the layers of the GM, and (III) the desorption from GM or partitioning between the lower surface of the GM and the lower component of the landfill liner, such as geosynthetic clay liners and compacted clay liners (Eun et al., 2018; Foose et al., 2002). The sorption process from the landfill leachate to the upper layer of the GM can involve incorporation into the microvoids of the GM, formation of clusters, solvation-shell cell formation, and other modes of mixing (Rowe, 2005; Sangam and Rowe, 2001). These processes depend on the chemical interaction between the polymer and the permanent contaminant (Nefso and Burns, 2007). Partition and diffusion coefficients of organic contaminants including benzene, methylene chloride (MC), trichloroethylene (TCE), and tertiary butyl ether (MTBE) of HDPE GMs have been extensively studied (Eun et al., 2018). The partition

* Corresponding author.
E-mail addresses: aahmad33@gmu.edu (A. Ahmad), ktian@gmu.edu (K. Tian), btanyu@gmu.edu (B. Tanyu), gfoster@gmu.edu (G.D. Foster).

https://doi.org/10.1016/j.wasman.2023.11.015
Received 16 June 2023; Received in revised form 9 October 2023; Accepted 13 November 2023
Available online 22 November 2023

coefficient of TCE is 69.02 L/kg, whereas the MTBE is 0.82 L/kg (Eun et al., 2018). The MTBE has a lower partition coefficient on GM than that of TCE because MTBE is an ether and the structure contains an oxygen atom in the middle of the carbon chain imparting it a bent structure in comparison to TCE which has a linear structure. The diffusion coefficient of MTBE and TCE have been reported as 7.74×10^{-13} m^2/s and 5.45×10^{-13} m^2/s respectively (Park et al., 2012). The greater diffusion coefficient of MTBE can be attributed to both its lower molecular mass as well as its non-halogenated structure. The diffusion of organic contaminants decreases with increasing molar mass and the structure and shape of a contaminant molecule also affect the diffusion (Saleem et al.,1989). Chlorinated hydrocarbons (e.g. TCE) had lower sorption on HDPE GMs than aromatic hydrocarbons (e.g., benzene), however, the diffusion of TCE was faster than that of benzene. (Rowe, 2005; Sangam and Rowe, 2001).

Per-polyfluoroalkyl substances (PFAS) are emerging organic contaminants and have become a rising concern for landfill facilities. PFAS are highly recalcitrant fluoro organic contaminants (Buck et al., 2011). PFAS are (1) thermally and chemically very stable, (2) acidic, and (3) hydrophobic and lipophobic surfactants (CONCAWE, 2016; Henry et al., 2018; Krafft and Riess, 2015). Classification of PFAS is based on functional groups, carbon chain lengths, and structural forms. The major groups amongst the Per-fluoroalkyl substances (fully fluorinated) include perflourocarboxylic acids (PFCAs), perfluorosulfonic acids (PFSAs), and perfluorosulfonamides (FOSAs). Poly-fluoroalkyl substances (partially fluorinated) include groups like fluorotelomer sulfonic acids (FtSAs) and fluorotelomer alcohols (FTOHs). Recent regulations have led to the synthesis/production of sub-groups like perfluoroalkane sulfonamidoacetic acids (FOSAA) and GenX (Ammonium perfluoro (2-methyl-3-oxahexanoate)). Gen X is an ether carboxylic acid with 6 carbons. While most PFAS are straight-chained, Gen X possesses an asymmetrical structure with a fluoroalkyl chain (C_3-F_7–) which is bonded on one side of an oxygen atom at the apex and a fluoroalkane carboxyl group on the other side (C_3-F_4COO^+–). PFAS are widely used in the production of domestic and industrial products, including fabrics, food packaging, water-repellent paints, carpets, upholstery, and non-stick cookware (Buck et al., 2011; Henry et al., 2018; KEMI, 2015; Schaider et al., 2017). Fluoroplastics, composite resins, aqueous fire-fighting filming foams (AFFF), and semiconductor industries have been also reported to use PFAS for manufacturing processes (Barzen-Hanson et al., 2017; Glüge et al., 2020; Lohmann et al., 2020). MSW landfills serve as the final disposal site for domestic waste and are considered a hotspot of PFAS. Lang et al. (2017) reported that 70 PFAS compounds from 14 classes of PFAS compounds have been found in the leachates from municipal solid waste (MSW) landfills in the U.S. with concentrations varying from 250 ng/L to 3500 ng/L. The classes of PFAS investigated by Lang et al. (2017) included PFCAs, PFSAs, FtSAs, FOSA, NMeFOSAAs, NEtFOSAA, 3 sub-classes of fluorotelomer carboxylic acids (FTCAs), fluorotelomer unsaturated carboxylic acids (FTUCAs), disubstituted polyfluorinated phosphate ester (DiPAP), Bisphosphates (DiSAmPAP), disubstituted perfluoroalkyl phosphinic acid (PFPIA), and fluorotelomer mercaptoalkyl phosphate ester (FTMAP). Another study by Gallen et al. (2017) found that the concentration of PFAS ranged from 73 to 25000 ng/L in the leachates based on an analysis of 27 MSW landfills in Australia. MSW leachate samples collected from four sites in northern Spain also contained a total of 1378.9 ng/L in untreated leachate. (Fuertes et al., 2017). Yan et al. (2015) found that PFOA accounted for 36.8 % of the total concentration of PFAS, which ranged from 7280 to 292,000 ng/L in landfill leachate collected from 5 MSW leachates in China.

So far limited information is available in the literature on the migration of PFAS through HDPE GM. Di Battista et al. (2020) studied the diffusion and partitioning of PFOA and PFOS in 0.1- and 0.75-mm linear low-density polyethylene (LLDPE) GMs using double-compartment column and batch sorption tests, respectively. K_d of PFOA and PFOS onto LLDPE ranged between 0.9 and 1.4 and 2.8 to 5.3, respectively. The diffusion coefficient of PFOA was measured in LLDPE, and the values were found to be $< 3.1 \times 10^{-16}$ m^2/s, $< 13 \times 10^{-16}$ m^2/s, and $< 19 \times 10^{-16}$ m^2/s at 23, 35, and 50 °C, respectively, whereas for PFOS the measured values were found to be $< 3.2 \times 10^{-16}$ m^2/s, $< 40 \times 10^{-16}$ m^2/s, and $< 52 \times 10^{-16}$ m^2/s at 23, 35, and 50 °C (Di Battista et al., 2020). The diffusion coefficients of PFOA and PFOS may be even lower because of the greater tortuosity through the amorphous crystalline nature of HDPE GMs compared to LLDPE (Di Battista et al., 2020).

The objective of our study was to quantify the partition and diffusion coefficients of selected PFAS in HDPE GM and to understand how these parameters are affected by changing the physiochemical properties of PFAS (molar mass and functional group/structure). The partition coefficients were evaluated for six different classes of PFAS (i.e., PFCAs, PFSAs, FOSAAs, FtSAs, FOSA, and Gen X) with HDPE GM whereas the diffusion coefficients were measured for PFCAs and PFSAs. The parameters were then used to predict the PFAS diffusive flux through intact HDPE GM, which yielded insight into the effectiveness of HDPE GMs as part of the composite liner systems for the containment of PFAS.

2. Materials and methods

2.1. Materials

A smooth 0.1-mm HDPE GM was used in this study. The engineering properties including thickness, puncture resistance, tear resistance, and tensile strength were measured according to ASTM D5944, ASTM D4833, ASTM D1004, and ASTM D6693 (Astm, 2013a; Astm, 2013b; Astm, 2015a; Astm, 2015b) respectively. All HDPE GM specimens were washed with DI water, before testing, to clean any impurities/dust present on the surface. The puncture and tear resistance were found to be 36.5 and 13.3 N respectively whereas 1.31 kN/m tensile strength at the yield point was observed with a 54.4 % elongation. A tensile strength of 1.56 kN/m corresponding to a 264 % elongation was observed at the breakpoint.

Fourier-transform infrared analysis (FTIR) analysis was also conducted on HDPE GM samples to characterize the surface functional groups. FTIR tests were conducted using the Agilent Cary 630 FTIR spectrometer, which uses the attenuated total reflection (ATR) spectroscopy method. The range of the wave numbers collected IR spectra varied from 4000 to 365 cm^{-1} and had a resolution of 4 cm^{-1}. The spectrometer has a single-reflection diamond, 1 mm diameter sampling surface with 200 μm active area. The spectrometer provides a penetration of approximately 2 μm for infrared energy at 1700 cm^{-1}. A specimen size of 25 mm x 25 mm was used and these specimens were subjected to uniform pressure in the ATR sampling module to ensure a high-quality spectrum. The transmittance values observed indicated the presence of alcohol (–OH), alkane (–CH), ketone(–CO), aromatic (C = C), and sulphoxide (S = O) groups.

2.2. Static batch experiments

Static batch tests were conducted to measure the partition coefficients of PFAS on the 0.1-mm HDPE GM, according to procedures outlined in Park et al. (2012), and Eun et al. (2018). Twenty-four PFAS were investigated in this study, including six classes: PFCAs, PFSAs, FOSAAs, FtSAs, FOSA, and Gen X. The selected PFAS can be classified based on carbon chain length, functional group, and structure. The number of carbons of these PFAS ranged from C-4 to C-14 and comprised of both partially and fully fluorinated PFAS. Functional groups include carboxylic acid, sulphonic acid, sulphonamide acetic acids, sulfonamides, and ether carboxylic acids. The structures of these PFAS have partially and fully fluorinated straight-chained compounds but also include one bent structure (Gen X). The CAS No., acronyms, formulae, number of carbons in the chain, molar weight, and functional groups of these selected PFAS are shown in Table 1.

PFAS solutions were prepared using Milli-Q Type I water to a target

Table 1
Physical properties of selected PFAS.

Name	CAS No.	Acronym	Formula	Carbon Chain Length	Mol. Wt. (g/mol)	Functional Group Classification
Perfluorobutanoic acid	375–22-4	PFBA	$C_4HF_7O_2$	4	214.04	Perfluoroalkyl Carboxylic Acids[2]
Perfluoropentanoic acid	2706–90-3	PFPeA	$C_5HF_9O_2$	5	264.05	
Perfluorohexanoic acid	307–24-4	PFHxA	$C_6HF_{11}O_2$	6	314.06	
Perfluoroheptanoic acid	375–85-9	PFHpA	$C_7HF_{13}O_2$	7	364.06	
Perfluorooctanoic acid	335–67-1	PFOA	$C_8HF_{15}O_2$	8	414.07	
Perfluorodecanoic acid	335–76-2	PFDA	$C_{10}HF_{19}O_2$	10	514.09	
Perfluoroundecanoic acid	2058–94-8	PFUnA	$C_{11}HF_{21}O_2$	11	564.1	
Perfluorododecanoic acid	307–55-1	PFDoA	$C_{12}HF_{23}O_2$	12	614.10	
Perfluorotridecanoic acid	72629–94-8	PFTrDA	$C_{13}HF_{25}O_2$	13	664.11	
Perfluorotetradecanoic acid	376–06-7	PFTeDA	$C_{14}HF_{27}O_2$	14	714.12	
N-methyl Perfluorooctane sulfonamidoacetic acid	2355–31-9	NMeFOSAA	$C_{11}H_6F_{17}NO_4S$	11	571.21	N-alkyl Perfluoroalkane Sulfonamidoacetic Acids
N-ethyl Perfluorooctane sulfonamidoacetic acid	2991–50-6	NEtFOSAA	$C_{12}H_8F_{17}NO_4S$	12	585.23	
Perfluorobutane sulfonic acid	375–73-5	PFBS	$C_4HF_9O_3S$	4	300.10	PerfluoroalkaneSulfonic Acids[1]
Perfluoropentane sulfonic acid	2706–91-4	PFPeS	$C_5HF_{11}O_3S$	5	350.10	
Perfluorohexane sulfonic acid	355–46-4	PFHxS	$C_6HF_{13}O_3S$	6	400.11	
Perfluoroheptane sulfonic acid	375–92-8	PFHpS	$C_7HF_{15}O_3S$	7	450.12	
Perfluorooctane sulfonic acid	1763–23-1	PFOS	$C_8HF_{17}O_3S$	8	500.13	
Perfluorononane sulfonic acid	68259–12-1	PFNS	$C_9HF_{19}O_3S$	9	550.14	
Perfluorodecane sulfonic acid	335–77-3	PFDS	$C_{10}HF_{21}O_3S$	10	600.14	
1H,1H,2H,2H-perfluorohexane sulfonic acid	757124–72-4	4:2 FtSA	$C_6H_5F_9O_3S$	6	328.15	Fluorotelomer Sulfonic Acids
1H,1H,2H,2H-perfluorooctane sulfonic acid	27619–97-2	6:2 FtSA	$C_8H_5F_{13}O_3S$	8	428.17	
1H,1H,2H,2H-perfluorodecane sulfonic acid	39108–34-4	8:2 FtSA	$C_{10}H_5F_{17}O_3S$	10	528.18	
Perfluorooctane sulfonamide	754–91-6	FOSA	$C_8H_2F_{17}NO_2S$	8	499.14	Perfluoroalkane Sulfonamide
Ammonium perfluoro (2-methyl-3-oxahexanoate)	62037–80-3	GenX	$C_6H_4F_{11}NO_3$	6	347.08	Gen X

[1]Diffusion coefficient was only measured for C-4, C-6 and C-8 PFSAs
[2]Diffusion coefficient was only measured for C-4 through C-10, C-12 and C-14 PFCAs.

concentration of 200, 400, 600, and 800 μg/L. The pH of the solutions was close to neutral (e.g., 6.7 to 6.9). HDPE GM specimens were cut into strips with a total mass of 0.4 g and added to 10 mL of multi-solute PFAS solutions in a 15 mL Falcon polypropylene tube. Polypropylene vials were then sealed and placed in a rotator and tumbled at a speed of 60 rpm for 8 days. This equilibration process was carried out at ambient laboratory temperature, which ranged between 20 and 25 °C. The 8-day time to reach equilibrium was chosen based on the equilibration time observed in initial trials. Duplicate tests were conducted.

At the end of the equilibration time, the HDPE GM strips were carefully removed, and the polypropylene vials were centrifuged at 2000 rpm for 20 mins to ensure homogeneity of the PFAS solution. The supernatant from each test vial was filtered sequentially using 0.2-μm polypropylene syringe filters with glass syringes from Fisher Scientific (Waltham, Massachusetts), followed by 0.05-μm Polyether sulfone (PES) syringe filters from Tisch Scientific (Cleves, Ohio). To prevent any potential contamination, all reusable glassware was pre-rinsed with methanol. 0.4-mL of the collected filtrate was diluted (1:1) in methanol and spiked with calibration standards and analyzed using liquid chromatography-tandem mass spectrometry (LC-MS/MS), as described in a later section. Each experiment was conducted in triplicate to ensure accuracy and consistency. To verify whether there was any contamination or interaction between the PFAS and the container walls, control tests were carried out using 15-mL Falcon tubes with 10 mL of multi-PFAS solutions at each concentration. The K_d (L/Kg) or (mL/g) was calculated using equation (1) shown below, as the ratio between the concentration of a contaminant sorbed in the GM (C_s in nmol/g) and its concentration in the aqueous phase at equilibrium (C_{eq} in nmol/mL). C_{eq} values were directly determined by LC-MS/MS.

$$K_d = \frac{C_s}{C_{eq}} \tag{1}$$

The corresponding concentrations of PFAS sorbed by HDPE GM were calculated as the difference from the initial test concentration. Linear fitting was used to fit the sorption isotherms and a least squares fitting of the sorption isotherms was performed with the Solver function in Microsoft Excel™ to find the set of adjustable parameters that minimized the root mean square error.

2.3. Kinetic batch experiments

Kinetic batch tests were conducted on the 0.1-mm HDPE GM to measure the diffusion coefficient of 11 PFAS (PFCAs and PFSAs). The kinetic batch test method was adopted from Park et al., (2012), and Eun et al., (2018). Like the static batch tests, the HDPE GM samples were cut into strips with a mass of approximately 0.4 g which were placed in 15-mL Falcon tubes containing 10 mL of multi-solute PFAS solutions. Each PFAS compound yields.

a concentration of 300 μg/L. Duplicate vials were decommissioned, and samples were collected daily from day 1 to day 8. The PFAS concentration data was analyzed by assuming a planar HDPE GM sheet, which was initially free of solutes and was suspended with both sides exposed in a well-stirred solution of fixed volume and mass. The diffusion coefficients were obtained based on the analytical solution by Crank (1975):

$$\frac{C_t}{C_o} = exp\left(\frac{D_g t(K_d)^2}{A^2}\right) erfc\left(\frac{D_g t(K_d)^2}{A^2}\right)^{0.5} \tag{2}$$

where C_t = concentration of the PFAS in the solution [ML^{-3}] at time t [T]; C_0 = initial concentration of solute in the solution [ML^{-3}]; D_g = diffusion coefficient [L^2T^{-1}] in the geomembrane; K_d = partition coefficient; and A = half thickness of the solution in contact with both sides of the geomembrane [L], which is calculated by dividing the volume of the solution by the area of the geomembrane.

2.4. LC-MS/MS analysis

A Shimadzu 8050 LC-MS/MS (Shimadzu, Columbia, MD) was used to analyze all samples for the 24 PFAS. The instrument is equipped with dual Nexera 20ADXR UHPLC pumps, SIL-20ACXR autosampler, and a C18 Restek Raptor Column (50 mm x 2.1 mm, 1.8 µm particle dia). A flow rate of 0.4 mL/min was maintained during analyses. 5 mM ammonium acetate in water (A) and 5 mM ammonium acetate in methanol (B) were used as the mobile phases. The mobile phases' gradient elution followed 0.10 min 90 % A, 1.00 min 70 % A, 9.00 min 30 % A, 9.50 min 5 %, 10.00 5 % A, 10.10 min 90 % A, 13.10 min 90 % A. The temperature of the C18 column was set at 40 °C. A capillary voltage of 2.8 kV, cone gas flow rate of 50 L/h, desolvation gas flow rate of 100 L/h, source temperature at 120 °C, and desolvation temperature at 400 °C were set as the main working parameters for the MS detector. Nitrogen (99.9 %) was used as cone gas and argon (99.9 %) was used as collision gas. Negative electrospray ionization and MRM detection modes were used to analyze all PFAS compounds whereas the identification was performed using 3 characteristic MRM ions, the first of which (MRM-1) was used for quantification.

Internal injection standard (IS) method and an eight-point calibration curve was used to perform calibration. According to USEPA method 537 (USEPA, 2020), the calibration curves were forced through the origin. Internal standards (IS) were checked for target suppression while the percentage recovery in sorption tests was evaluated using surrogate standards (SS). High-purity (96 % or better) analytical standards were used for calibration. Analytical standards were procured as single compounds from Wellington Laboratories (Guelph, Ontario, Canada) in 1.2 mL glass ampules. These standards include a total of six individual isotopically labeled standards (3 x IS and 3 x SS). 13C2 perfluorooctanoic acid (13C2-PFOA), 13C4 perfluorooctanesulfonate (13C4-PFOS) and d3-N-methyl perfluorooctane-sulfonamido acetic acid (d3-N-MeFOSAA) were used as IS, whereas 13C2 perfluorohexanoic acid (13C2-PFHxA), 13C2 perfluorodecanoic acid(13C2MPFDA) and d5-N-ethyl perfluorooctane-sulfonamido acetic acid (d5-N-EtFOSAA) were used as SS.

2.5. Quality assurance

To reduce sample contamination, polypropylene labware was pre-rinsed with methanol. Blanks of HDPE GM samples were also run to confirm any contribution to the measured concentration of target compounds. Additionally, the same tubes and conditions were used to run control tests. The results indicated that the material used did not cause notable compound losses or degradation due to PFAS sorption. Additionally, the method's reproducibility was determined by calculating the relative standard deviation of triplicate sample analyses and found to be within a reasonable range of 5–15 %.

3. Results and discussion

3.1. Effect of molar mass and number of carbons in chain on partition coefficients

The K_d of PFCAs and PFSAs versus the molar mass/number of carbons in the chain for the HDPE GM evaluated in this study are shown in Fig. 1. The K_d of PFCAs is shown in Fig. 1(a). K_d of C-4 to C-7 are similar, ranging from 5.1 to 6.4 L/kg. An increasing trend with increasing molar mass on the HDPE GM is observed from C-8 to C-14. The K_d for PFCAs showed little variation from C-4 to C-7, with an average value of 5.7 L/kg with the highest value of 6.4 L/kg observed for PFHxA (C-6). A gradual increase in K_d was observed from C-7 to C-10. Thereafter, a steep increase in K_d was observed from C-10 to C-14 from 12.5 L/kg for PFDA (C-10) to the highest value observed at 90.4 L/kg for PFTeDA (C-14).

Fig. 1(b) presents the K_d values of PFSAs determined in this study as a function of the molar mass/number of carbons in the chain for HDPE GM. The trend observed for PFSAs is similar to PFCAs, i.e., K_d of shorter chained PFAS (e.g., C4-C7) are similar, whereas an increase in molar mass leads to a steep increase in K_d from C-8 onwards. The K_d increased from 8.8 L/kg to 98.3 L/kg as the number of carbons increase of PFAS increased from C-4 to C-10.

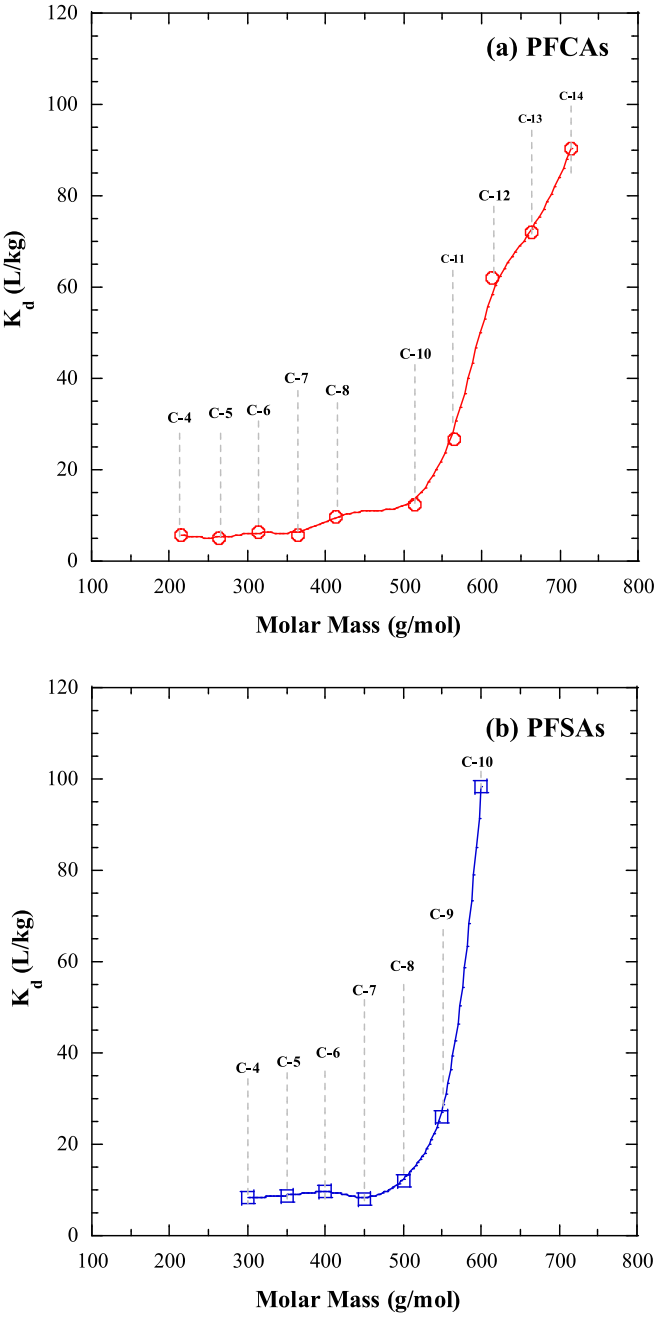

Fig. 1. Partitioning coefficients (K_d) determined in this study of (a) PFCAs, and (b) PFSAs with HDPE GM as a function of molar mass.

The K_d of FOSAAs, FtSAs, FOSA, and Gen X have been tabulated in Table 2. NMeFOSAA and NEtFOSAA exhibit K_d of 62.3 and 77.4 L/kg respectively. Among FtSAs an increasing trend of K_d with molar mass was also observed with values of 3.8, 10.1, and 30.8 L/kg observed for C-6, C-8, and C-10 respectively. FOSA had a K_d of 57.1 L/kg whereas Gen X exhibited a K_d of 5.6 L/kg.

The sorption of PFAS is dependent on the molecular mass (number of carbons) because increasing molecular mass yields a reduction in surface area to volume ratio and hence, results in greater Van der Waals forces amongst its molecules (Atkins et al., 2017) These temporary

Table 2
Partition and diffusion coefficients of PFAS with HDPE GM.

Name	Acronym	K_d (L/Kg)	D_g (m^2/s)
Perfluorobutanoic acid	PFBA	5.8	4.67 x 10^{-17}
Perfluoropentanoic acid	PFPeA	5.1	4.18 x 10^{-17}
Perfluorohexanoic acid	PFHxA	6.4	2.67 x 10^{-17}
Perfluoroheptanoic acid	PFHpA	5.8	1.35 x 10^{-17}
Perfluorooctanoic acid	PFOA	9.8	1.30 x 10^{-17}
Perfluorodecanoic acid	PFDA	12.5	5.30 x 10^{-18}
Perfluoroundecanoic acid	PFUnA	26.6	–
Perfluorododecanoic acid	PFDoA	62.0	6.44 x 10^{-18}
Perfluorotridecanoic acid	PFTrDA	71.9	–
Perfluorotetradecanoic acid	PFTeDA	90.4	1.04 x 10^{-18}
N-methyl Perfluorooctane sulfonamidoacetic acid	NMeFOSAA	62.3	–
N-ethyl Perfluorooctane sulfonamidoacetic acid	NEtFOSAA	77.4	–
Perfluorobutane sulfonic acid	PFBS	8.3	2.81 x 10^{-17}
Perfluoropentane sulfonic acid	PFPeS	8.8	–
Perfluorohexane sulfonic acid	PFHxS	9.8	2.28 x 10^{-17}
Perfluoroheptane sulfonic acid	PFHpS	8.2	–
Perfluorooctane sulfonic acid	PFOS	12.1	6.42 x 10^{-18}
Perfluorononane sulfonic acid	PFNS	26.0	–
Perfluorodecane sulfonic acid	PFDS	98.3	–
1H,1H,2H,2H-perfluorohexane sulfonic acid	4:2 FtSA	3.8	–
1H,1H,2H,2H-perfluorooctane sulfonic acid	6:2 FtSA	10.1	–
1H,1H,2H,2H-perfluorodecane sulfonic acid	8:2 FtSA	30.8	–
Perfluorooctane sulfonamide	FOSA	57.1	–
Ammonium perfluoro (2-methyl-3-oxahexanoate)	GenX	5.6	–

dipoles of PFAS lead to greater hydrophobicity (repulsion from the aqueous phase) and increase the chance of physical interaction with the structure of the HDPE GM. A similar observation has also been previously reported for chlorinated hydrocarbons, where it was observed that the sorption of 1,2-dichloroethane (1,2-DCA) (C-2) is higher than the sorption of di-chloroethane (DCM) (C-1) on HDPE GM (Sangam and Rowe, 2001).

3.2. Effect of functional group and structure on partition coefficients

Fig. 2 shows the K_d of fifteen PFAS with HDPE GM. These PFAS have been categorized into five different groups according to the number of carbons in the chain (C-6, C-8, C-10, C-11, and C-12 PFAS). The results illustrate that PFAS structure (e.g., fluorine saturation and bent structure vs. linear structure) and functional group (e.g., carboxyl vs. sulfonic vs. sulfonamide) affect the sorption on HDPE GM.

3.2.1. Functional group

The functional group of PFAS affects the K_d on HDPE GM, i.e., carboxyl vs. sulfonic vs. sulfonamide. For example, PFHxA ($C_6HF_{11}O_2$) and PFHxS ($C_6HF_{13}O_3S$) have a similar number of carbons in the chain but consist of different terminal functional groups, but the K_d of PFHxS is 52.2 % higher than that of PFHxA (9.8 L/kg vs. 6.4 L/kg). Similarly, the K_d of PFOS ($C_8HF_{17}O_3S$) is 12.1 L/kg, whereas the K_d of PFOA ($C_8HF_{15}O_2$) is 9.8 L/kg, as shown in Fig. 2. The greatest impact of the terminal functional group on the K_d can be observed for the C-10 s

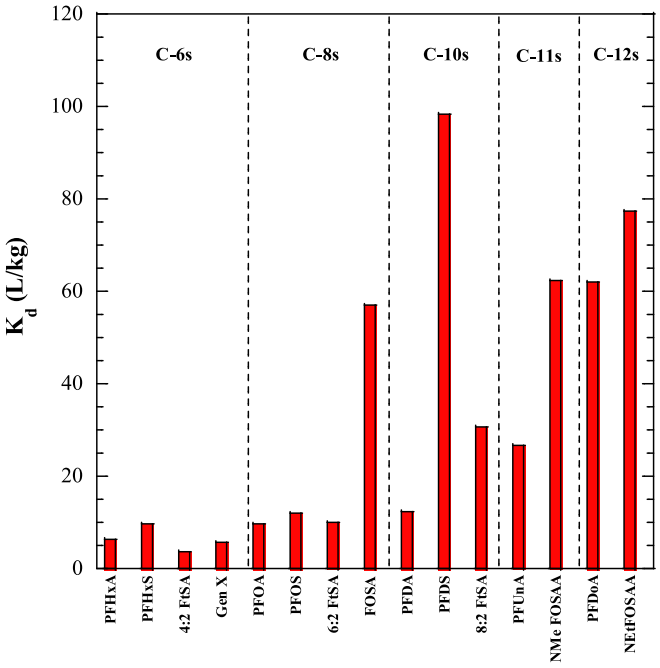

Fig. 2. Partitioning coefficients (K_d) determined in this study of C-6, C-8, C-10, C-11, and C-12 PFAS on HDPE GM as a function of PFAS functional groups.

(PFDA and PFDS), where the K_d of PFDS is 98.3 L/kg vs. 12.5 L/kg of PFDA. The higher sorption of PFSAs is because the sulphonic acid functional group has a greater hydrophobicity than the carboxylic functional group (Xing et al., 2020). The higher hydrophobicity of the PFSAs than PFCAs at a similar total number of carbons is due to the presence of an extra carbon atom in the chain/tail of a PFSA in comparison to a PFCA and leads to greater sorption on HDPE GM.

In terms of the sulfonamide functional group, NEtFOSAA has the highest K_d amongst the C-8 PFAS. PFOS, PFOA, and FOSA which are structurally analogous except for the addition of a nitrogen ion in the sulphonic functional group making it a sulfonamide ion. For FOSAAs, the total number of carbons are eleven and twelve (carbon tail has eight carbons hence grouped with C-8 s) as the functional group has additional three and four carbons, respectively, for NEtFOSAA and NMeFOSAA. The effect of the functional group and structure together can be observed. The K_d of FOSAAs is higher than FOSA. The sulfonamide functional group imparts a higher hydrophobicity to the PFAS molecule in comparison to the sulphonic group, hence, making it more nonionic in an aqueous environment and yielding a higher interaction with the sorbent structure (Wang et al., 2015). The K_d generally is highest with sulfonamide followed in order by sulphonic and carboxylic function groups.

3.2.2. PFAS structure

PFHxS and 4:2 FtSA have a similar number of carbons in chain and functional groups, however, the K_d of PFHxS is 9.8 L/kg whereas the 4:2 FtSA has a K_d of 3.8 L/kg. This observation can be attributed to the degree of fluorine saturation. PFHxS has 6 fully fluorinated carbon atoms, whereas 4:2 FtSA has 4 fully saturated carbon atoms. Similar observation can be made for the C-8 and C-10 PFAS with a similar number of carbons in the chain but different fluorine saturation. The K_d of 6:2 FtSA is 17 % lower than the K_d of PFOS of 12.1 L/kg whereas the K_d of PFDS (10 fluorinated carbons) is 98.25 L/Kg in comparison to 30.8 L/kg for 8:2FtSA (8 fluorinated carbons). In FtSAs there are more hydrogen atoms (less fluorination) on the chain structure, while a C–H bond is weaker than C-F, and hydrogen has a smaller Van der Waals radius, which make FtSAs relatively less hydrophobic than PFSAs. A similar trend had previously been observed for the degree of

chlorination (halogenation). Sangam and Rowe, (2001) reported TCE (3 chorines) to sorb stronger to HDPE GM than 1,2-DCA (2 chlorines) and concluded that a greater degree of halogenation in organic contaminants potentially yields higher sorption on HDPE GM.

The effect of PFAS structure can also be observed for Gen X, which is a bent structure compared to the other linear C-6 PFAS. Gen X (C-6) compound exhibits a K_d of 5.6 L/kg, which is lower than PFHxA (e.g., 6.4 L/kg), with a similar number of carbons in chain, and PFHxS (9.8 L/kg), but higher than 4:2 FtSA. Similar findings were reported in the literature that MTBE with an ether structure has a much smaller K_d (0.82 L/kg) than that of TCE (liner structure) (69.02 L/kg) on HDPE GM (Eun et al., 2018). Ethers with a partially negative oxygen atom at the apex and a relatively smaller surface area yield a relatively higher solubility (Gen X has the highest solubility in C-6 PFAS) and hence lower sorption on sorbents. K_d depends on the structure of the PFAS and generally increases with the degree of fluorination.

The sorption mechanism of PFAS on HDPE GM can potentially be governed by processes that include, incorporation into microvoids, formation of clusters, and solvation-shell cell formation. These processes depend on the chemical interaction between the polymer chains of HDPE GM and the fluorocarbon chain (tail) of the PFAS molecules. Incorporation into the microvoids of HDPE GM is a physical process that potentially occurs due to the hydrophobic interaction (repulsion) of the non-polar PFAS chain with the polar water molecules. The formation of clusters and solvation shells are due to the attractive forces that are generated between the PFAS non-polar body and the HDPE GM polymers when both come in contact. Van der Waals forces can potentially be generated due to the electron cloud fluctuations caused by the high electronegativity of the fluorine atoms present in the PFAS. The electron cloud fluctuations cause the formation of weak dipoles and create an attraction between the two non-polar surfaces. These interactions between PFAS and HDPE GM have been illustrated in Fig. 3. The size and geometry of the micropores in polyethylene were studied by Shanbhag et al. (1990) and reported that interconnected voids ranging between 160 and 368 μm were present in polyethylene and more than half of the pores were larger than 150 μm in diameter. The molecular size of PFAS varies in the order of nanometers (Xiao et al., 2012). The size of PFAS molecules is much smaller than the pore size of the voids in present in HDPE GM therefore little to no effect on sorption of PFAS is expected due to the porosity of the HDPE GM.

3.3. Diffusion coefficients of PFCAs and PFSAs

The D_g of 11 PFAS (PFCAs and PFSAs) were determined from kinetic batch tests. As an example, the measured relative concentration (C_t/C_o) profile of PFOA (C-8) as a function of time is shown in Fig. 4. The D_g

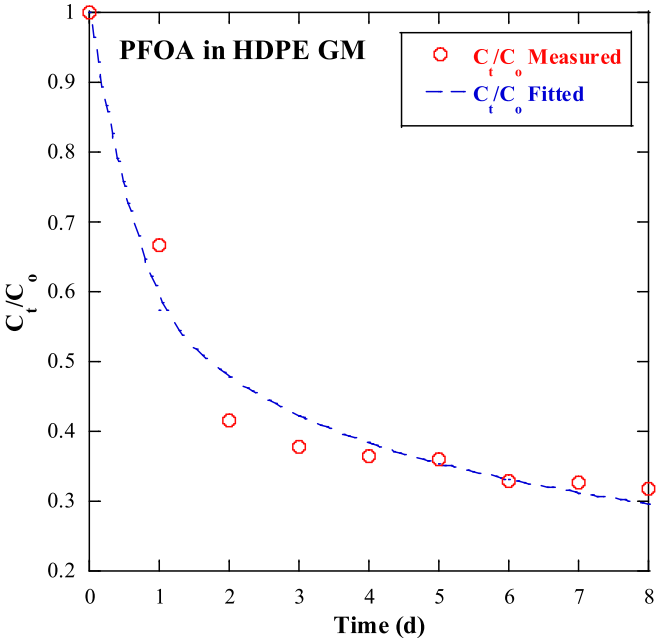

Fig. 4. Example fitting of relative concentration versus time for determination of diffusion coefficient (D_g) for PFOA(C-8).

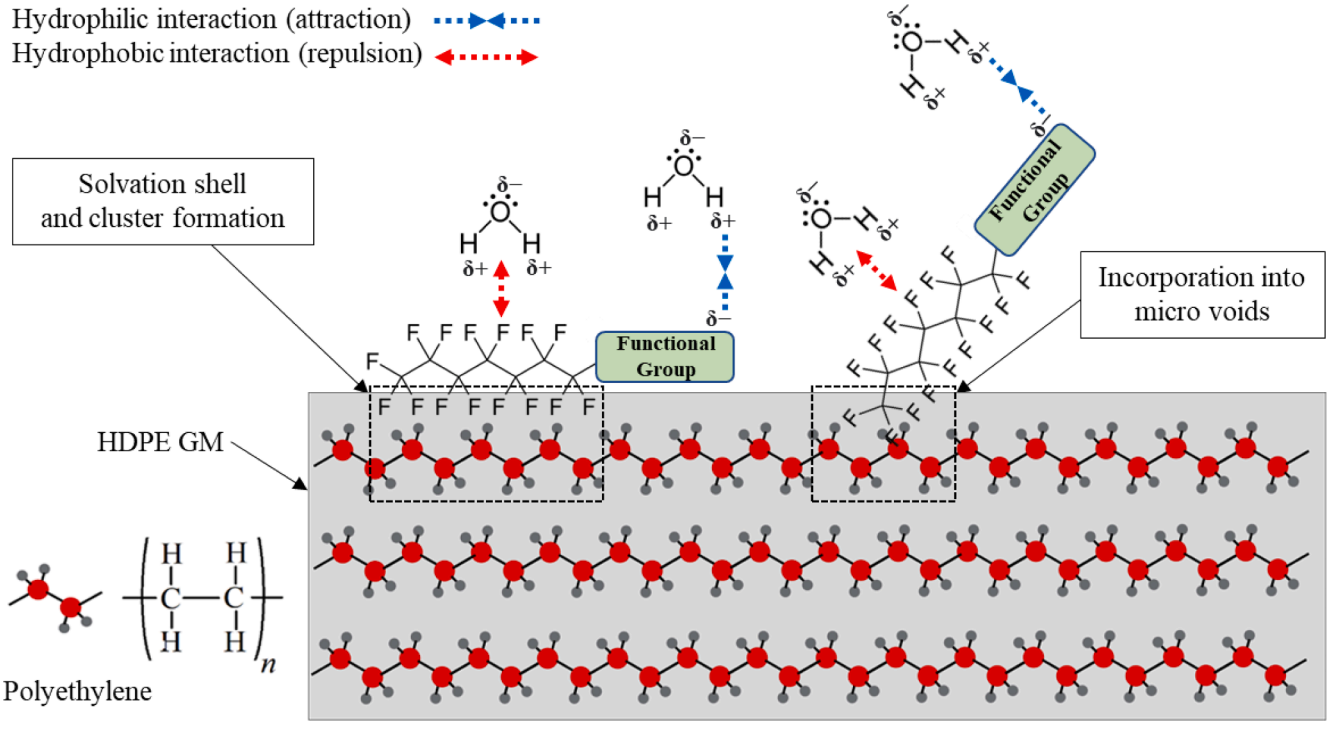

Fig. 3. Sorption mechanism of PFAS on HDPE GM.

were obtained by fitting the relative concentration curve data from the kinetic batch tests with equation (2) using non-linear squares regression with the Solver tool in Microsoft Excel. The fittings for different PFAS were made by solving only for the value of D_g while the measured values of K_d were used from the results of the static batch sorption tests.

The D_g of PFCAs and PFSAs in 0.1-mm HDPE GM are shown in Fig. 5. Generally, a decreasing trend of D_g was observed for all PFAS with increasing molar mass (number of carbons in the chain). The D_g of PFBA (C-4) was observed to be 4.67×10^{-17} m^2/s which decreased to a value of 1.30×10^{-17} m^2/s for PFOA (C-8). The D_g of PFDA (C-10) was observed to be 5.30×10^{-18} m^2/s which is lower than PFOA however the D_g observed for PFDoA (C-12) was slightly higher than PFDA. The lowest D_g amongst PFCAs was observed for PFTeDA (C-14) as 1.04×10^{-18} m^2/s. A similar decreasing trend was also seen for PFSAs where the values of D_g observed for PFBS (C-4), PFHxS (C-6), and PFOS (C-8) were 2.81×10^{-17} m^2/s, 2.28×10^{-17} m^2/s, and 6.42×10^{-18} m^2/s respectively.

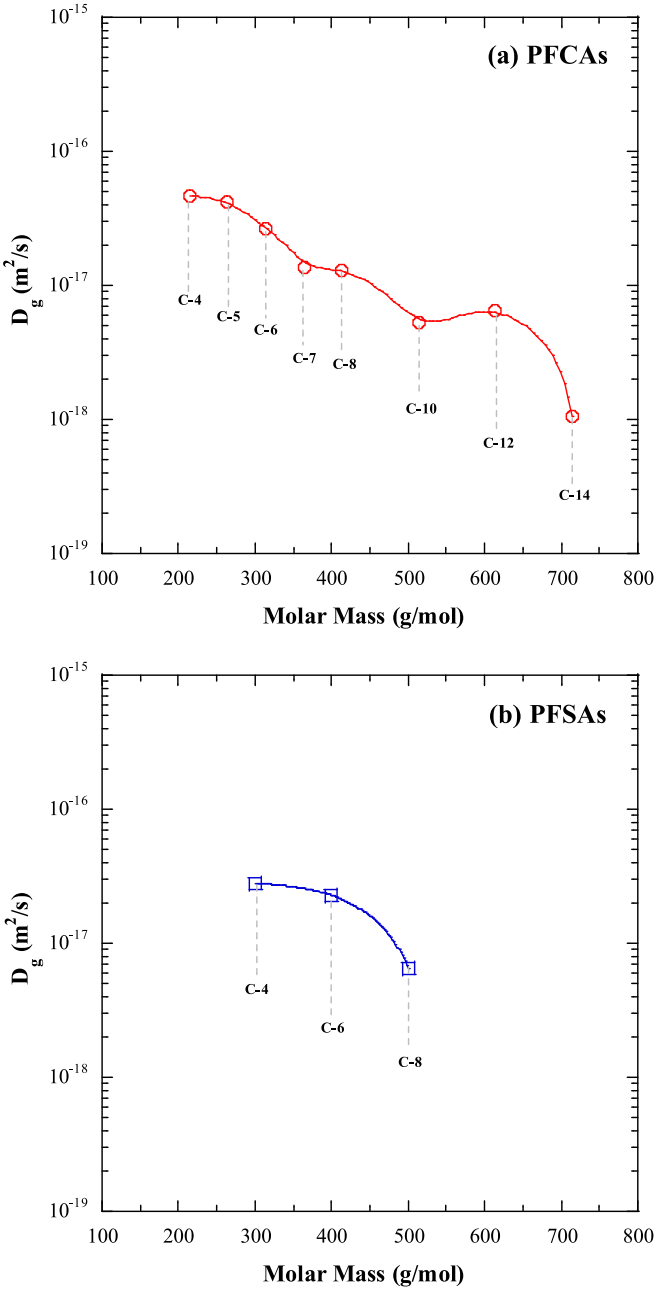

Fig. 5. Diffusion coefficients (D_g) determined in this study of (a) PFCAs, and (b) PFSAs in HDPE GM as a function of molar mass.

The effect of the functional group on the D_g can also be observed. At a similar number of carbons in the chain, the D_g for PFSAs was found to be lower than that of PFCAs, e.g., PFOS has a D_g of 6.42×10^{-18} m^2/s whereas PFOA has a D_g of 1.30×10^{-17} m^2/s (6.58×10^{-18} m^2/s lower). Similar findings were observed for C-6 (PFHxS and PFHxA) and C-4 (PFBS and PFBA), as shown in Table 2. The larger molecular mass of PFSA molecules, coupled with higher sorption potentially reduces the permeation through the HDPE GM structure yielding lower diffusion coefficients than PFCAs. The D_g generally decreases with increasing molar mass/no of carbons in chain, and at similar no of carbons in chain a lower value of D_g was observed for PFSAs than PFCAs.

3.4. Diffusive flux through GM

The diffusive flux and estimated breakthrough times for 11 PFAS (PFCAs and PFSAs) have been tabulated in Table 3. These values were calculated for intact 1.5-mm HDPE GM (which are typically used as landfill liners) using equations (3) and (4). Once a contaminant reaches equilibrium and a concentration develops on the surface or within the GM, the sorbed contaminant starts to diffuse through the GM. The diffusion through a GM can be expressed by Fick's first law:

$$J_d = -D_g \frac{dC_g}{dx} \tag{3}$$

where J_d is the diffusive flux, D_g is the diffusion coefficient, C_g is the sorbed concentration on the GM surface calculated as the product of K_d and C_o (leachate concentration) and x is the direction of diffusive transport (Sangam and Rowe, 2001). The time of breakthrough at steady state can be calculated by using a simplified form of a one-dimensional diffusion advection equation (Rowe et al., 2004) as shown as follows:

$$t = z^2/D_g \tag{4}$$

For estimation purposes, the concentration of the PFAS in a hypothetical leachate was assumed to be 4000 ng/L. The K_d and D_g were measured for 0.1-mm HDPE GM and can be used for flux calculation because Nefso and Burns (2007) investigated the sorption of organic compounds with HDPE GMs of thickness and reported no significant difference in uptake.

The flux of PFCAs varied from 38.7 ng/m^2/year to 2080.8 ng/m^2/year whereas the flux of PFSAs varied from 79.6 to 182.9 ng/m^2/year. The estimated breakthrough times for PFCAs have a minimum value of 1526 years for PFBA and this value increases with an increasing number of carbons in the chain. The breakthrough times for PFSAs had the least value of 2538 years for PFBS (higher than the PFBA with a similar number of carbons). The D_g were determined at ambient laboratory temperatures varying between 20 and 25 °C. The temperatures observed in MSW landfills can reach up to 80 °C which leads to the degradation of the HDPE GM (Rowe, 2005; Rowe et al., 2009). The reduction in crystallinity of HDPE GM causes an increase in porosity and hence increases

Table 3
Flux and breakthrough time of selected PFAS in intact 1.5 mm HDPE GM.

Name	Acronym	Flux (ng/m^2/year)	Breakthrough time (years)
Perfluorobutanoic acid	PFBA	130.5	1526.21
Perfluoropentanoic acid	PFPeA	89.7	1704.95
Perfluorohexanoic acid	PFHxA	92.4	2672.02
Perfluoroheptanoic acid	PFHpA	38.7	5294.18
Perfluorooctanoic acid	PFOA	105.9	5485.77
Perfluorodecanoic acid	PFDA	69.5	13457.08
Perfluorododecanoic acid	PFDoA	2080.8	11083.98
Perfluorotetradecanoic acid	PFTeDA	717.8	68338.60
Perfluorobutane sulfonic acid	PFBS	163.0	2538.43
Perfluorohexane sulfonic acid	PFHxS	182.9	3130.74
Perfluorooctane sulfonic acid	PFOS	79.6	11110.84

the diffusion coefficients of the permeant organic contaminants. Rowe and Barakat, (2021) reported a breakthrough time of 425 years for PFOS for HDPE GM based on elevated temperature tests (50 °C). A time of 660 years for PFOS diffusion in 0.1-mm LLDPE was also reported for room temperature testing (Di Battista et al., 2020). These breakthrough times are relatively large compared to the typical operation and post-closure monitoring time for MSW landfill liners. However, the estimated values of flux and breakthrough times based on measured K_d and D_g suggest that intact HDPE GMs would provide excellent containment against the migration of PFAS in landfills. Further study is ongoing to predict the migration of PFAS through composite liner systems considering liner defects (e.g., holes and damages).

4. Conclusions

PFAS migration through landfill liners is currently a particular area of concern for landfill owners, regulators, and geo-environmental engineers. HDPE GMs are a critical component of MSW landfill liners to prevent contaminants from leaching out to the environment. Sorption and diffusion are two important mechanisms that potentially dictate the contaminants to pass through HDPE GMs. In this study, static and kinetic batch tests were conducted to measure the partition and diffusion coefficients of PFAS migrating through HDPE GM. A total of 24 PFAS with varying number of carbons in the chain and functional groups have been investigated. The results demonstrate that all classes of PFAS investigated (PFCAs, PFSAs, FOSAAs, FTSAs, FOSA, and Gen X) tend to sorb onto HDPE GM and can diffuse through HDPE GM.

Sorption of all PFAS was observed on 0.1-mm HDPE GM. The partition coefficient ranged from 3.8 to 98.3 L/kg. The partition coefficients are not sensitive to the molar mass/number of carbons in the chain for shorter PFAS (e.g., C4 to C7), however, a direct relationship of partition coefficients is observed with the molar mass of PFAS for longer-chained PFAS (C-8 and longer).

The partition coefficient was also observed to be dependent on the functional group and structure of the PFAS. The Sulfonamide functional group (FOSA, FOSAAs) had the strongest sorption followed by sulphonic (PFSAs) and carboxylic acids (PFCAs) because of the difference in hydrophobicity of the different PFAS functional groups. The structure in terms of the degree of fluorine saturation in linear sulphonic acids affected the partition coefficient. Lower sorption was observed for the partially saturated fluorotelomer sulphonic acids (FtSAs) compared to the perfluoro sulphonic acids (PFSAs). The single Gen X (ether carboxylic acid) had a partition coefficient value smaller than other C-6 fully fluorinated straight chained PFAS because of its bent structure.

The diffusion coefficients of PFAS in HDPE GMs varied in order (increasing number of carbons in chain) from 1.04×10^{-18} m^2/s to 4.67×10^{-17} m^2/s for PFCAs and 6.42×10^{-18} m^2/s to 2.81×10^{-17} m^2/s for PFSAs. The diffusion coefficients showed an inverse relationship with an increase in molar mass/number of carbons in the chain (e.g., PFBA has a diffusion coefficient of 4.67×10^{-17} m^2/s whereas PFTeDA has 1.04×10^{-18} m^2/s). The diffusion coefficients of PFSAs were smaller than PFCAs for similar number of carbons (C-8) in the chain (e.g., PFOS has a diffusion coefficient of 6.42×10^{-18} m^2/s whereas PFOA has 1.30×10^{-17} m^2/s).

The estimated breakthrough times of PFAS through intact 1.5-mm HDPE GMs are more than 1500 years based on the partitioning and diffusion coefficients (determined in this study) and show HDPE GMs to be excellent barriers against PFAS migration. Further study is needed to predict the migration of PFAS through composite liner systems considering liner defects (e.g., holes and damages).

Declaration of Competing Interest

The authors declare that they have no known competing financial interests or personal relationships that could have appeared to influence the work reported in this paper.

Data availability

The data that has been used is confidential.

References

Aminabhavi, T.M., Naik, H.G., 1998. Chemical compatibility testing of geomembranes – sorption/desorption, diffusion, permeation and swelling phenomena. Geotext. Geomembr. 16 (6), 333–354. https://doi.org/10.1016/S0266-1144(98)00017-X.

ASTM. (2013a). "Standard test method for index puncture resistance of geomembranes and related products." ASTM D4833 M-07, West Conshohocken, PA.

ASTM. (2013b). "Standard test method for tear resistance (graves tear) of plastic film and sheeting." ASTM D1004-13, West Conshohocken, PA.

ASTM. (2015a). "Standard test method for determining tensile properties of nonreinforced polyethylene and nonreinforced flexible polypropylene geomembranes." ASTM D6693 M-04, West Conshohocken, PA.

ASTM. (2015b). "Standard test method for measuring core thickness of textured geomembranes." ASTM D5944 M-10, West Conshohocken, PA .

Atkins, P.J., De Paula, J., Keeler, J., 2017. Atkins' physical chemistry, (11th ed.). Oxford University Press.

August, H., Taztky, R., 1984. "In: Permeability of commercial available polymeric liners for hazardous landfill leachate organic constituents.". International Conference on Geomembrane, Denver, USA 151–156.

Barzen-Hanson, K.A., Davis, S.E., Kleber, M., Field, J.A., 2017. Sorption of fluorotelomer sulfonates, fluorotelomer sulfonamido betaines, and a fluorotelomer sulfonamido amine in national foam aqueous film-forming foam to soil. Environ. Sci. Tech. 51 (21), 12394–12404. https://doi.org/10.1021/acs.est.7b03452.

Buck, R.C., Franklin, J., Berger, U., Conder, J.M., Cousins, I.T., Voogt, P.D., Jensen, A.A., Kannan, K., Mabury, S.A., van Leeuwen, S.P.J., 2011. Perfluoroalkyl and polyfluoroalkyl substances in the environment: Terminology, classification, and origins. Integr. Environ. Assess. Manag. 7 (4), 513–541. https://doi.org/10.1002/ieam.258.

Concawe, 2016. Environmental Fate and Effects of Poly- and Perfluoroalkyl Substances (PFAS). Auderghem, Belgium https://www.concawe.eu/publication/environmental-fate-and-effects-of-poly-and-perfluoroalkyl-substances-pfas-report-no-816/.

Crank, J., 1975. The mathematics of diffusion, 2nd Ed. Clarendon, Oxford, U.K., pp. 56–60

Di Battista, V., Rowe, R.K., Patch, D., Weber, K., 2020. PFOA and PFOS diffusion through LLDPE and LLDPE coextruded with EVOH at 22 °C, 35 °C, and 50 °C. Waste Manag. 117, 93–103. https://doi.org/10.1016/j.wasman.2020.07.036.

Eun, J., Tinjum, J.M., Benson, C.H., Edil, T.B., 2018. Equivalent transport parameters for volatile organic compounds in coextruded geomembrane-containing ethylene-vinyl alcohol. J. Geotech. Geoenviron. Eng. 144 (7), 1–14. https://doi.org/10.1061/(asce)gt.1943-5606.0001888.

Foose, G.J., Benson, C.H., Edil, T.B., 2002. Comparison of solute transport in three composite liners. J. Geotech. Geoenviron. Eng. 128 (5), 391–403. https://doi.org/10.1061/(asce)1090-0241(2002)128:5(391).

Fuertes, I., Gómez-Lavín, S., Elizalde, M.P., Urtiaga, A., 2017. Perfluorinated alkyl substances (PFASs) in northern Spain municipal solid waste landfill leachates. Chemosphere 168, 399–407. https://doi.org/10.1016/j.chemosphere.2016.10.072.

Gallen, C., Drage, D., Eaglesham, G., Grant, S., Bowman, M., Mueller, J.F., 2017. Australia-wide assessment of perfluoroalkyl substances (PFASs) in landfill leachates. J. Hazard. Mater. 331, 132–141. https://doi.org/10.1016/j.jhazmat.2017.02.006.

Glüge, J., Scheringer, M., Cousins, I.T., Dewitt, J.C., Goldenman, G., Herzke, D., Lohmann, R., Ng, C.A., Trier, X., Wang, Z., 2020. An overview of the uses of per- And polyfluoroalkyl substances (PFAS). Environ. Sci. Processes Impacts 22 (12), 2345–2373. https://doi.org/10.1039/d0em00291g.

Henry, B.J., Carlin, J.P., Hammerschmidt, J.A., Buck, R.C., Buxton, L.W., Fiedler, H., Seed, J., Hernandez, O., 2018. A critical review of the application of polymer of low concern and regulatory criteria to fluoropolymers. Integr. Environ. Assess. Manag. 14 (3), 316–334. https://doi.org/10.1002/ieam.4035.

Hsuan, Y.G., Koerner, R.M., 1995. The single point-notched constant load test: A quality control test for assessing stress crack resistance. Geosynth. Int. 2 (5), 831–843. https://doi.org/10.1680/gein.2.0038.

Kemi, 2015. Occurrence and use of highly fluorinated substances and alternatives. Swedish Chemicals Agency Report 7/15D.

Koerner, G.R., Koerner, R.M., 2006. Long-term temperature monitoring of geomembranes at dry and wet landfills. Geotext. Geomembr. 24 (1), 72–77. https://doi.org/10.1016/j.geotexmem.2004.11.003.

Krafft, M.P., Riess, J.G., 2015. Selected physicochemical aspects of poly- and perfluoroalkylated substances relevant to performance, environment and sustainability—Part one. Chemosphere 129, 4–19. https://doi.org/10.1016/j.chemosphere.2014.08.039.

Lang, J.R., Allred, B.M.K., Field, J.A., Levis, J.W., Barlaz, M.A., 2017. National estimate of per- and polyfluoroalkyl substance (PFAS) release to U.S. Municipal landfill leachate. Environ. Sci. Tech. 51 (4), 2197–2205. https://doi.org/10.1021/acs.est.6b05005.

Lohmann, R., Cousins, I.T., DeWitt, J.C., Glüge, J., Goldenman, G., Herzke, D., Lindstrom, A.B., Miller, M.F., Ng, C.A., Patton, S., Scheringer, M., Trier, X., Wang, Z., 2020. Are fluoropolymers really of low concern for human and environmental health and separate from other PFAS? Environ. Sci. Tech. 54 (20), 12820–12828. https://doi.org/10.1021/acs.est.0c03244.

Nefso, E.K., Burns, S.E., 2007. Comparison of the equilibrium sorption of five organic compounds to HDPE, PP, and PVC geomembranes. Geotext. Geomembr. 25 (6), 360–365. https://doi.org/10.1016/j.geotexmem.2006.12.002.

Park, M.G., Benson, C.H., Edil, T.B., 2012. Comparison of batch and double compartment tests for measuring voc transport parameters in geomembranes. Geotext. Geomembr. 31, 15–30. https://doi.org/10.1016/j.geotexmem.2011.09.001.

Rowe, R.K., 2005. Long-term performance of contaminant barrier systems. Geotechnique 55 (9), 631–678. https://doi.org/10.1680/geot.2005.55.9.631.

Rowe, R.K., Barakat, F.B., 2021. Modelling the transport of PFOS from single lined municipal solid waste landfill. Comput. Geotech. 137 (June), 104280. https://doi.org/10.1016/j.compgeo.2021.104280.

R. Rowe L. Hrapovic M.D. Armstrong *Diffusion of organic pollutants through HDPE geomembrane and composite liners and its influence on groundwater quality*. 1996 737 742.

Rowe, R., Hrapovic, L., Kosaric, N., 1995. Diffusion of chloride and dichloromethane through an HDPE geomembrane. Geosynth. Int. 2 https://doi.org/10.1680/gein.2.0021.

Rowe, R.K., Rimal, S., Sangam, H., 2009. Ageing of HDPE geomembrane exposed to air, water and leachate at different temperatures. Geotext. Geomembr. 27 (2), 137–151. https://doi.org/10.1016/j.geotexmem.2008.09.007.

Saleem, M., Asfour, A.-F.-A., De Kee, D., Harrison, B., 1989. Diffusion of organic penetrants through low density polyethylene (LDPE) films: Effect of size and shape of the penetrant molecules. J. Appl. Polym. Sci. 37 (3), 617–625. https://doi.org/10.1002/app.1989.070370303.

Sangam, H.P., Rowe, R.K., 2001. Migration of dilute aqueous organic pollutants through HDPE geomembranes. Geotextiles and Geomembranes 19 (6), 329–357. https://doi.org/10.1016/S0266-1144(01)00013-9.

Schaider, L.A., Balan, S.A., Blum, A., Andrews, D.Q., Strynar, M.J., Dickinson, M.E., Lunderberg, D.M., Lang, J.R., Peaslee, G.F., 2017. Fluorinated compounds in U.S. Fast food packaging. Environmental Science & Technology Letters 4 (3), 105–111. https://doi.org/10.1021/acs.estlett.6b00435.

Shanbhag, A., Friedman, H.I., Augustine, J., von Recum, A.F., 1990. Evaluation of porous polyethylene for external ear reconstruction. Ann. Plast. Surg. 24 (1).

Tian, K., Benson, C.H., Tinjum, J.M., Edil, T.B., 2017. Antioxidant depletion and service life prediction for HDPE geomembranes exposed to low-level radioactive waste leachate. J. Geotech. Geoenviron. Eng. 143 (6), 1–11. https://doi.org/10.1061/(asce)gt.1943-5606.0001643.

Tian, K., Benson, C.H., Yang, Y., Tinjum, J.M., 2018. Radiation dose and antioxidant depletion in a HDPE geomembrane. Geotext. Geomembr. 46 (4), 426–435. https://doi.org/10.1016/j.geotexmem.2018.03.003.

USEPA. (2020). *537.1 - 1. 1* 2009 1 50.

Wang, F., Shih, K.M., Li, X.Y., 2015. The partition behavior of perfluorooctanesulfonate (PFOS) and perfluorooctanesulfonamide (FOSA) on microplastics. Chemosphere 119, 841–847. https://doi.org/10.1016/j.chemosphere.2014.08.047.

Xiao, F., Davidsavor, K.J., Park, S., Nakayama, M., Phillips, B.R., 2012. Batch and column study: Sorption of perfluorinated surfactants from water and cosolvent systems by Amberlite XAD resins. J. Colloid Interface Sci. 368 (1), 505–511. https://doi.org/10.1016/j.jcis.2011.11.011.

Xing, D.Y., Chen, Y., Zhu, J., Liu, T., 2020. Fabrication of hydrolytically stable magnetic core-shell aminosilane nanocomposite for the adsorption of PFOS and PFOA. Chemosphere 251, 126384. https://doi.org/10.1016/j.chemosphere.2020.126384.

Yan, H., Cousins, I.T., Zhang, C., Zhou, Q., 2015. Perfluoroalkyl acids in municipal landfill leachates from China: Occurrence, fate during leachate treatment and potential impact on groundwater. Sci. Total Environ. 524–525, 23–31. https://doi.org/10.1016/j.scitotenv.2015.03.111.